Saudi Journal of Biological Sciences 28 (2021) 3660–3668

Contents lists available at ScienceDirect

Saudi Journal of Biological Sciences

journal homepage: www.sciencedirect.com

Original article

Sunlight-driven rapid and facile synthesis of Silver nanoparticles using *Allium ampeloprasum* extract with enhanced antioxidant and antifungal activity

V. Uma Maheshwari Nallal [a], K. Prabha [b], I. VethaPotheher [c], Balasubramani Ravindran [d], Alaa Baazeem [e], Soon Woong Chang [d], Gloria Aderonke Otunola [f,*], M. Razia [a,*]

[a] Department of Biotechnology, Mother Teresa Women's University, Kodaikanal, Tamil Nadu, India
[b] Department of Physics, Mother Teresa Women's University, Kodaikanal, Tamil Nadu, India
[c] Department of Physics, University College of Engineering, Bharathidasan Institute of Technology Campus, Anna University, Tiruchirapalli, Tamil Nadu, India
[d] Department of Environmental Energy and Engineering, Kyonggi University, Youngtong – Gu, Suwon 16227, Republic of Korea
[e] Department of Biology, College of Science, Taif University, P.O. Box 11099, Taif 21944, Saudi Arabia
[f] Medicinal Plants and Economic Development (MPED) Research Center, Department of Botany, University of Fort Hare, Alice 5700, South Africa

ARTICLE INFO

Article history:
Received 8 April 2021
Revised 27 April 2021
Accepted 2 May 2021
Available online 13 May 2021

Keywords:
A. ampeloprasum
Sunlight
AgNPs
Antioxidant activity
Antifungal activity

ABSTRACT

Green nanotechnology has acquired immense demand due to its cost-effective, eco-friendly and benevolent approach for the synthesis of nanoparticles. Among the biological methods, plants aid as a significant green resource for synthesizing nanoparticles that are safe and non-toxic for human use. In the present investigation, Silver nanoparticles (AgNPs) were synthesized using bulbs extract of *Allium ampeloprasum* under the influence of sunlight irradiation and characterized using different techniques. Distinct *in-vitro* assays were performed to test the antioxidant and anticandida potential of the synthesized AgNPs. Results suggested the efficient and rapid sunlight-driven synthesis of AgNPs using *A. ampeloprasum* extract. UV–Vis spectrum showed absorption peak at 446 nm which confirmed the formation of AgNPs. FTIR analysis suggested the presence of functional groups associated with flavonoids and sulfur compounds in *A. ampeloprasum* extract. The synthesized AgNPs showed Face Centred Cubic (FCC) structure with an average size of 35 nm. Spherical, quasi spherical, triangular and ellipsoidal morphology of the NPs were observed from the TEM micrograph. The synthesized AgNPs showed pronounced free radical scavenging potential for DPPH, ABTS•+ and H_2O_2 radicals. The anticandida potency of the synthesized AgNPs was observed as follows: *C. albicans* ≥ *C. tropicalis* ≥ *C. glabrata* ≥ *C. parapsilosis* ≥ *C. krusei*. Results showed that sunlight driven nanoparticle synthesis of AgNPs is rapid, facile and exhibit enhanced antioxidant and antifungal activity.

1. Introduction

Eco-friendly and facile methods for nanoparticles synthesis with multi-faceted applications has revolutionized the field of modern medicine and technology (Shah et al., 2020). Interestingly among the metallic nanoparticles, Silver nanoparticles (AgNPs) have a wide range of applications and are synthesized up to 500 tonnes each year for biomedical uses (Al-Huqail et al., 2018). Biogenic syntheses of NPs are strongly addressed to be cost-effective, nature-friendly, rapid and facile when compared to chemical and physical methods. Among the bio-based methods for the synthesis of NPs, plant extract mediated synthesis has gained immense attention and appreciation due to its non-toxic attributes (Krishna et al., 2015). Fabrication of metallic NPs from microbial sources has its own advantages but the process of culturing and maintaining microbial cells is tedious and additional chemicals in the form of culturing media are indirectly involved in these methods. Moreover the toxicity of the intracellular and extracellular compounds produced by the microbial cells is

* Corresponding authors.
E-mail addresses: gotunola@ufh.ac.za (G.A. Otunola), razia581@gmail.com (M. Razia).
Peer review under responsibility of King Saud University.

Production and hosting by Elsevier

https://doi.org/10.1016/j.sjbs.2021.05.001
1319-562X/

ambiguous (Saravanan et al., 2017). The ease of plant-mediated synthesis of NPs is enhanced by the phytocompounds present in the plant extract that act as reducing and capping agents during the process. Considering the toxicity of the phytocompounds, the use of edible plants as green resource can yield NPs that are safe for human use (Ahmed et al., 2016).

Allium ampeloprasum (leek) is an edible vegetable under the genus *Allium* and is closely associated with onion (*A. cepa*) and garlic (*A. sativum*) (Abbas, 2019). *A. ampeloprasum* is rich in organosulfur compounds, particularly dominated by gamma glutamyl peptides rather than alliin and allicin (Ceccanti et al., 2020). This imparts a mild pungent smell and a sweet onion flavour to the leeks when compared to the strong pungent smell of onion and garlic. *A. ampeloprasum* is characterised by white shafts or bulbs and green leaves which are rich repositories of secondary metabolites such as polyphenols, phenolic acids, flavonoids and saponins (Lu et al., 2011). Najda et al., (2016) reports that *A. ampeloprasum* bulbs showed higher phenol concentration and antioxidant activities than common garlic bulbs. Lu et al., (2011) suggests that bulbs play an influential role in the secondary metabolite profile of the entire plant. *A. ampeloprasum* has been an important ingredient in European cuisines and Iranian folklore medicines (Rahimi-Madiseh et al., 2017). Several researchers have reported that *A. ampeloprasum* has anti-proliferative (An et al., 2015), anti-bacterial (Bareemizadeh et al., 2014), anti-fungal (Nallal et al., 2020), anti-ulcer (Adão et al., 2011), anti-diabetic (Rahimi-Madiseh et al., 2017), anti-oxidative (Nallal et al., 2020) and anti-inflammatory (Adão et al., 2011) effects through *in-vitro* and *in-vivo* assays. Novel steroidal saponins have been identified and elucidated in *A. ampeloprasum* extracts (Sobolewska et al., 2014). Based on nutritional values *A. ampeloprasum* has been less explored for its medicinal attributes and very few characterizations for novel metabolites in this edible plant has been performed till date. In this regard, the current study focuses on the sunlight-driven biogenic synthesis and characterization of AgNPs using the aqueous extract of *A. ampeloprasum* bulbs (AB) and its potential applications.

2. Materials and methods

2.1. Preparation of plant extract

A. ampeloprasum was procured from a native farmer at Kodaikanal, Tamilnadu. All the parts of plant were washed thoroughly in running tap water followed by double distilled water wash. The whites shafts or bulbs were separated from the leaves, chopped into small pieces are shade-dried for 15 days. 300 mg of the powdered bulbs was added to 35 mL of double distilled water in a 50 mL conical flask and the solution was boiled. The concoction was allowed to cool and filtered using Whatman's No1 filter paper (11 μm) and freshly used for the synthesis of AgNPs.

2.2. Sunlight-driven biosynthesis of AgNPs

25 mL of *A. ampeloprasum* bulb extract was added to 275 mL of 1 mM freshly prepared Silver nitrate ($AgNO_3$) solution. The concoction containing $AgNO_3$ and the fresh extract was mixed well and immediately exposed to sunlight irradiation (at a temperature of 18–20 °C). Biogenic synthesis of AgNPs using *A. ampeloprasum* bulb extract (AB AgNPs) was confirmed by the change in colour from pale yellow to dark brown within few minutes of exposure. Later the concoction was centrifuged at 12,000*g* for 20 min. The supernatant was discarded and the pellets were dispersed in sterile distilled water and washed thrice to remove the unreacted phyto-constituents. The pellets were dried at 37 °C and stored for further use (Saha and Bandyopadhyay, 2017).

2.3. Characterization of AgNPs

AB AgNPs were characterized using various techniques and instruments. The biogenic reduction of Silver ions in the concoction was periodically measured using a Shimadzu Ultra-Violet visible (UV–Vis) spectrophotometer at a range of 200–800 nm. Screening of functional groups was performed using Perkin Elmer spectrum 100 N Fourier Transform Infrared (FTIR) (4000–500 cm^{-1}). Crystalline nature of the AB AgNPs was analysed using a X' Pert Pro – Panalytic powder X-ray diffractometer (XRD) with Cu Kα radiation source and Ni filter operating at 30 mA, 40 kV and scanned over a 2θ range of 20–80°. Non-agglomeration tendency and stability of the NPs were measured using Zeta potential analysis (Malvern instruments Ltd; operating at 25 °C). Morphology of synthesized NPs were studied using High resolution Transmission Electron Microscopy (HR-TEM) (Joel/Jem 2100) with a voltage rate of 200 kV and 2000×–1,500,000× magnification.

2.4. Total phenol content (TPC) and total flavonoid content (TFC) of AB AgNPs

2.4.1. Determination of TPC by Folin-ciocalteu method

The total phenol content in AB AgNPs was determined by Folin-ciocalteu method. To 1 mL of different concentrations of AB AgNPs (2, 4, 6, 8 and 10 μg/mL) 0.5 mL of Folin-ciocalteu reagent was added and the mixture was vortexed. To this 2.5 mL of 5% Sodium carbonate solution was added and incubated for 30 min at room temperature. The absorbance was measured using a Shimadzu spectrophotometer at 725 nm. Different aliquots of Gallic acid was used as the standard to plot the calibration curve and the results were expressed as Gallic acid equivalents (mg GAE/g) (Haq et al., 2012).

2.4.2. Determination of TFC by Aluminium chloride method

Total flavonoids content in AB AgNPs was determined by Aluminium chloride method ($AlCl_3$). To 1 mL of different concentrations of AB AgNPs (2, 4, 6, 8 and 10 μg/mL) 2 mL of $AlCl_3$ was added. To this mixture 6 mL of Sodium acetate was added and mixed well. The absorbance was measured using a Shimadzu spectrophotometer at 430 nm. Different aliquots of Quercetin was used as the standard to plot the calibration curve and the results were expressed as Quercetin equivalents (mg QE/g) (Chang et al., 2002).

2.5. Free radical scavenging capacity and antioxidant activity of AB AgNPs

2.5.1. DPPH free radicals scavenging assay

To determine the DPPH free radical scavenging capacity of AB AgNPs, different concentrations of AB AgNPs (2, 4, 6, 8 and 10 μg) were taken. To this 2 mL of 0.1 mM DPPH solution in methanol was added and the mixture was incubated in dark for 30 min. The absorbance of the samples was measured at 517 nm (Manzocco et al., 1998). Different concentrations of Ascorbic acid were used as the control and the percentage of free radical scavenging was calculated as follows:

$$\% \text{ DPPH radicals scavenging} = \frac{(\text{Absorbance of Control} - \text{Absorbance of Sample}) \times 100}{\text{Absorbance of Control}}$$

2.5.2. ABTS•+ free radicals scavenging assay

To evaluate the ABTS•+ free radical scavenging ability of AB AgNPs, 7 mM of ABTS•+ was dissolved in double distilled water

to which 140 mM of potassium persulfate solution was added. The mixture was incubated in dark for 14 h and before the experiment they were diluted to give an absorbance of 0.700 ± 0.02 at 734 nm. Various concentrations (2, 4, 6, 8 and 10 μg/ mL) of AB AgNPs were mixed with the diluted ABTS•+ solution and incubated for 10 min. The measurements were taken at 734 nm and Ascorbic acid was used as the control (Seeram et al., 2006). The free radical scavenging ability was calculated as follows:

% ABTS•+ radicals scavenging = (Absorbance of Control–Absorbance of Sample) × 100
Absorbance of Control

2.5.3. Hydrogen peroxide radicals scavenging assay

To investigate the hydrogen peroxide scavenging activity different concentrations of (2, 4, 6, 8 and 10 μg/ mL) of AB AgNPs were taken. To this 0.6 mL of 40 mM hydrogen peroxide solution was added and mixed well. After 10 min the absorbance of the reaction mixture was measured at 230 nm and Ascorbic acid was used as the standard (Ruch et al., 1989). The hydrogen peroxide radical scavenging ability of AB AgNPs was calculated as follows:

% H_2O_2 radicals scavenging = (Absorbance of Control–Absorbance of Sample) × 100
Absorbance of Control

2.5.4. Nitric oxide radicals scavenging assay

To determine the Nitric oxide scavenging ability of AB AgNPs, different concentrations of AB AgNPs (2, 4, 6, 8 and 10 μg/mL) was taken. To this 10 mM of Sodium nitroprusside was added and incubated at 37 °C. 3 mL of Griess reagent was added to the mixture after incubation and the absorbance was measured at 546 nm. Ascorbic acid was used as the control (Amalraj et al., 2020). The nitric oxide radical scavenging activity was calculated as follows:

% Nitric oxide radicals scavenging = (Absorbance of Control-Absorbance of Sample) × 100
Absorbance of Control

2.5.5. Superoxide anions scavenging assay

Nitroblue tetrazolium (NBT) reduction assay was performed to determine the Superoxide anion scavenging ability of AB AgNPs. The reaction mixture for this assay was prepared by dissolving 20 μg riboflavin, 0.1 mg NBT and 12 mM EDTA in 50 mM in sodium phosphate buffer. 3 mL of this reaction mixture is added to various concentrations (2, 4, 6, 8 and 10 μg/mL) of AB AgNPs. The mixture was incubated at room temperature for 10 min and the absorbance was measured at 590 nm (Amalraj et al., 2020). Ascorbic acid was used as the control and the superoxide anion scavenging ability was measured as follows:

% Superoxide anion scavenging = (Absorbance of Control-Absorbance of Sample) × 100
Absorbance of Control

2.5.6. Metal chelating activity

To determine the metal chelating activity of AB AgNPs, 2 mM ferric chloride solution and 5 mM of ferrozine was added to different concentrations (2, 4, 6, 8 and 10 μg/ mL) of AB AgNPs. The reaction mixture was mixed thoroughly and left at 37 °C for 10 min. Ascorbic acid was used as the standard and the absorbance was measured at 562 nm. The metal chelating activity was expressed as EDTA equivalent (mg EDTA/g) (Amalraj et al., 2020).

2.5.7. Phosphomolybdenum assay

The total antioxidant capacity of AB AgNPs was determined by Phosphomolybdenum assay. The reaction mixture for this assay was prepared using 0.6 M sulphuric acid, 4 mM ammonium molybdate and 28 mM sodium phosphate. To different concentrations (2, 4, 6, 8 and 10 μg/ mL) of AB AgNPs 1 mL of the reaction mixture was added and incubated at 95 °C for 90 min in a water bath. Once the reaction solution was cooled the absorbance was measured at 765 nm and Ascorbic acid was used as the control. The results were expressed as Ascorbic acid equivalents (mg AAE/g) (Prieto et al.,1999).

2.6. Determination of anticandida activity of AB AgNPs

The anticandida activity of AB AgNPs was tested against five Candida strains (*C. albicans*- MTCC 183, *C. tropicalis*- MTCC 184, *C. glabrata*- MTCC 3019, *C. parapsilosis*- MTCC 7043 and *C. krusei*- MTCC 9215). Candida strains were procured from Microbial Type Culture Collection and Gene Bank (MTCC), Chandigarh, India. The method of Mallmann et al. (2015) with slight modifications was used. Candida cultures were preserved in Potato Dextrose Agar (PDA) slant at 4 °C. The inoculum was prepared by picking a single candida colony from PDA slant with a sterile loop and transferred to Potato Dextrose Broth (PDB) and incubated overnight in incubator cum shaker at 35 °C. The optical density of the candida culture suspensions were adjusted to 0.5 McFarland standards. Individual inoculum would contain approximately 10^7 CFU/mL.

2.6.1. Agar well diffusion assay

Agar well diffusion assay was done to establish the anticandida activity of AB AgNPs. Autoclaved PDA was prepared and poured into sterile petridishes. 0.1 mL of each candida strain was evenly swabbed on separate petridishes. Plates were allowed to air-dry for 10 min and later the wells were cut on the culture media and various concentrations of AB AgNPs (2.5–10 μg/mL) were pipetted in to each well. Amphotericin B was used as the standard antibiotic. The plates were incubated at 37 °C for 24 h. After 24 h, the zone of inhibition were examined and expressed in millimetres (Mallmann et al., 2015).

2.6.2. Determination of minimum inhibitory concentration (MIC)

The procured candida pathogens were inoculated in PDA slants at 37 °C. After 24 h, a single loop of test pathogens from the slant was transferred to 5 mL of sterile PDB and which was later adjusted to 0.5 McFarland scale. Two fold dilutions of AB AgNPs was added to the suspension medium, mixed well and incubated for 24 h at 37° C. MIC of the AgNPs was observed as the concentration at which more than 75% of the candida growth was inhibited in the broth. Amphotericin B was used as the standard antifungal agent (Balouiri et al., 2015).

3. Results

3.1. Sunlight-driven synthesis of AgNPs using A. ampeloprasum bulbs extract

Exposure of the mixture (plant extract + $AgNO_3$ solution) to sunlight irradiation resulted in immediate colour change. The mixture turned from pale yellow to dark brown within 20 min which confirmed the successful synthesis of AgNPs using *A. ampeloprasum* bulbs extract.

3.2. Characterization of AB AgNPs

3.2.1. Spectral analysis using UV–Vis spectroscopy

The UV–Visible spectrum of the solution was recorded at various time intervals such as 0, 5, 10, 15, 30 and 60 min. The colour change observed in the solution on exposure to the sunlight was due to the Surface Plasmon Resonance (SPR) phenomenon which refers to the vibration of the Silver ions. Fig. 1 illustrates the UV–Vis absorption peak within 446 nm and 450 nm range with respect to time lapse.

3.2.2. Spectral analysis of AB AgNPs using FTIR spectroscopy

The possible interactions between the Ag ions and the bioactive compounds in the reduction and capping of AB AgNPs were studied using FT-IR spectrometer. The FTIR spectrum of AB AgNPs is represented in Fig. 2. The band observed at 3438 cm^{-1} signified the OH stretch of alcohol or phenol group present in the bulbs extract. Peak at 1632 cm^{-1} corresponded to C=C alkene stretching, this functional group is predominantly studied in the flavonoids of plants. The band at 1416 cm^{-1} is related to C—H bending which corresponded to the proteins present in the extracts. Band at 1075 cm^{-1} represented very strong S=O stretching corresponding to the sulfoxides while bands at 624 cm^{-1} depicted S—H stretching that strongly suggests the presence of thiol groups. Vibrational peak for Ag was not observed since FTIR uses the mid-infrared ray (4000–400 cm^{-1}).

3.2.3. Analysis of the crystalline nature of AB AgNPs using XRD

Powder XRD analysis (Fig. 3) confirmed the crystalline nature of the photo-biosynthesized AB AgNPs. Diffraction peaks at 27.83°, 38.17°, 44.37°, 64.54°, 77.48° corresponded to (2 1 0), (1 1 1), (2 0 0), (2 2 0) and (3 1 1) planes of FCC structure of AgNPs synthesized from bulb extracts. The peaks at 32.28°, 32.34°, 46.27° and 46.38° arise from the presence of organic compounds in the bulb extract. The obtained powder XRD pattern was similar with JCPDS No 04-0783. The average particle size was calculated by using Debye-Scherrer formula

$$D = 0.9\lambda/\beta\cos\theta$$

Where, λ is the wavelength of the X-ray (0.1541), β is FWM (Full width half maximum), θ is the diffraction angle and D indicates the particle diameter size. The average particle size of AB AgNPs was calculated to be 35 nm.

3.2.4. Zeta potential analysis of AB AgNPs

Zeta potential analysis was performed to determine the extent of the electrostatic or charge repulsion/attraction between AB AgNPs. Zeta potential observed for the synthesized AB AgNPs was −23.3 mV (Fig. 4).

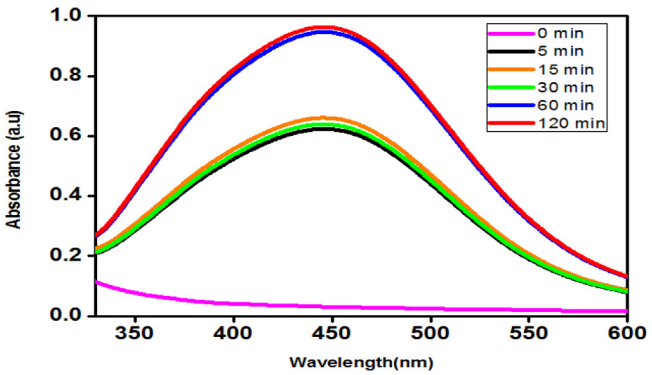

Fig. 1. UV–Vis spectrum of AB AgNPs synthesized under the influence of sunlight.

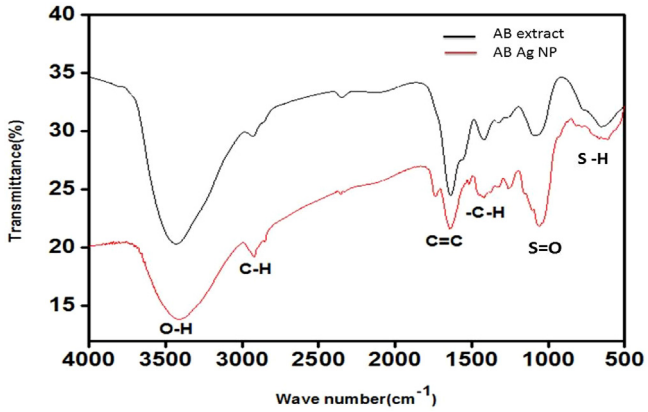

Fig. 2. FTIR spectrum of *A. ampeloprasum* bulb extract and AB Ag NPs.

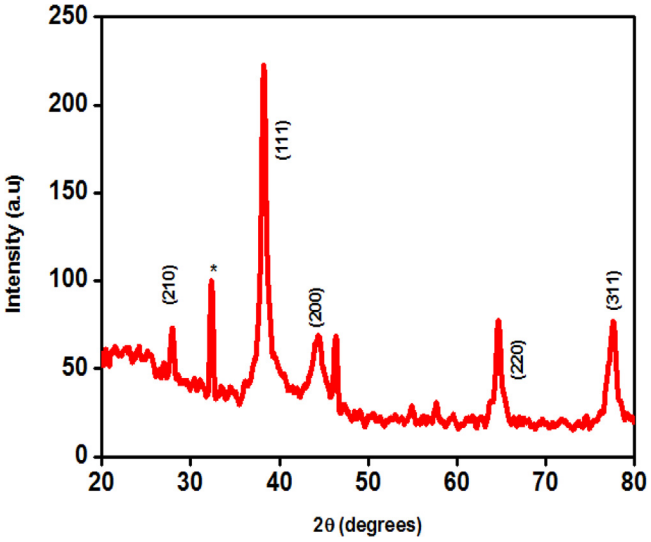

Fig. 3. XRD pattern of AB AgNPs that depicts the planes of FCC structure.

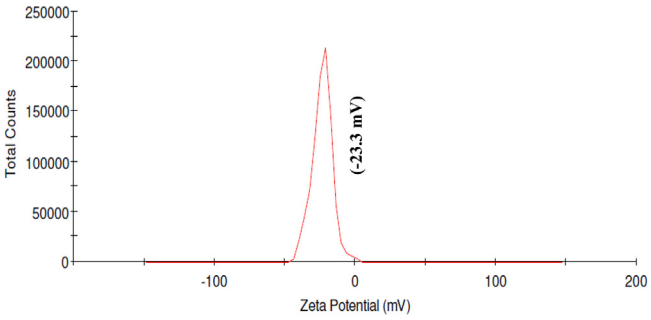

Fig. 4. Zeta potential analysis of AB AgNPs.

3.2.5. Identification AB AgNPs morphology using HRTEM

HRTEM analysis was performed to identify the surface morphology of AB AgNPs. The morphology was identified to be predominantly spherical and quasi spherical. Interestingly, ellipsoidal, triangular and hexagonal shapes (Fig. 5) were also observed. The interactions of the bioactive metabolites and organo sulphur compounds can act as important factors in determining the shape and size of the particles. The distance of the lattice plane was calculated as 0.18 nm for AB AgNPs using Bragg's law

$$2d\sin\theta = n\lambda$$

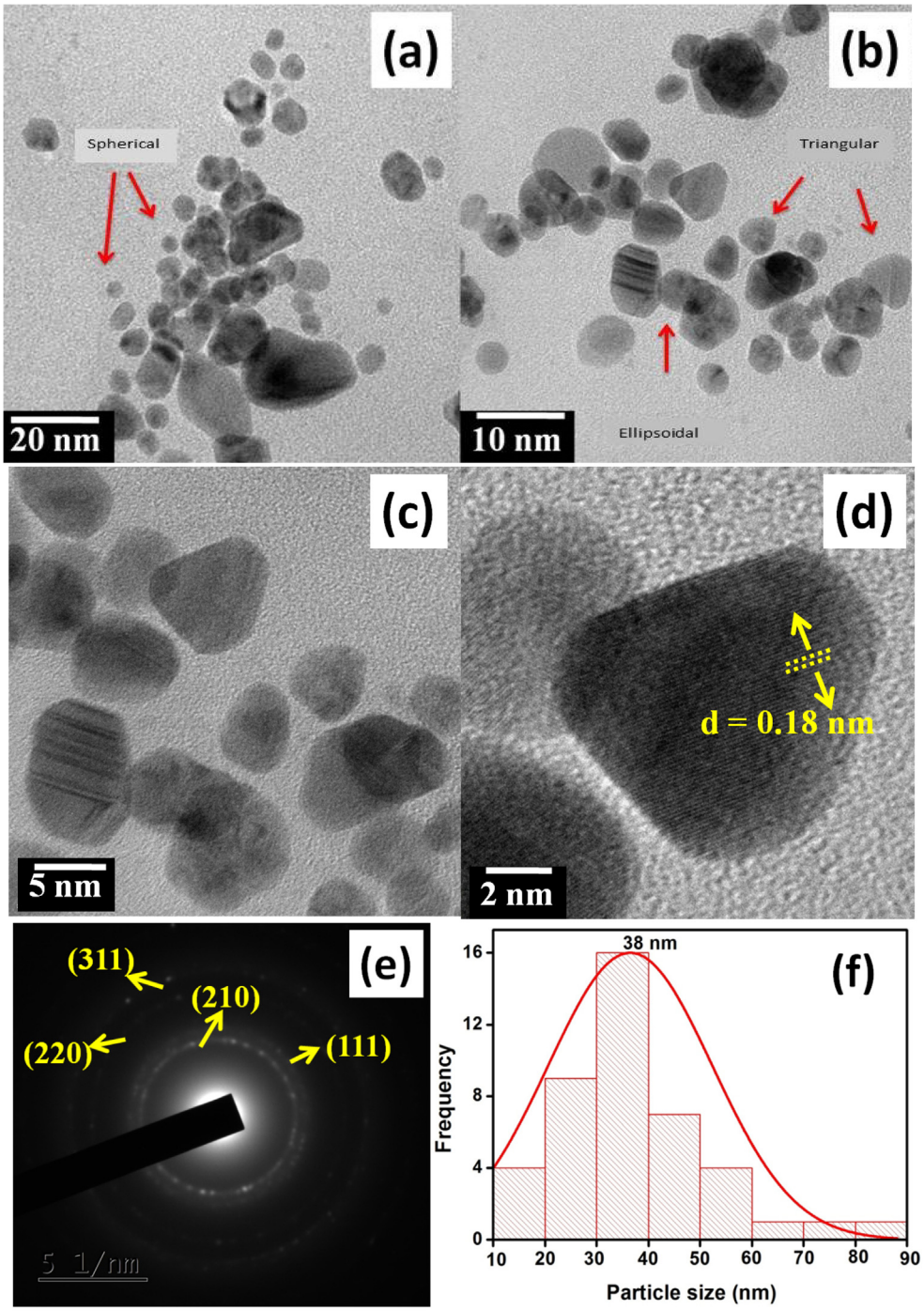

Fig. 5. TEM micrograph of AgNPs synthesized from AB extract at (a) 20 nm, (b) 10 nm, (c) 5 nm, (d) 2 nm, (e) SAED pattern, (f) Particle size histogram.

Where d is the interplanar spacing between the atoms, θ is the angle of incidence, n is a whole number; λ is the wavelength of the X-ray (0.1541 nm).

The obtained lattice spacing corresponds to the lattice spacing of the FCC phase of Ag. The SAED pattern of the AB AgNPs is shown in Fig. 5e. The obtained pattern can be correlated with the powder XRD and FCC nature, depicted by the bright spots corresponding to (2 1 0), (1 1 1), (2 0 0), (2 2 0) and (3 1 1) Braggs reflection planes. Additionally the particle size histogram shows that NPs ranging from 2 nm to 80 nm were synthesized in this study. The average size calculated from the histogram (Fig. 5f) was 38 nm which was close to the particle size calculated from the XRD results.

3.3. Total phenol and flavonoid content of AB AgNPs

TPC and TFC of AB AgNPs are represented in Table 1. It can be elucidated from the table that reasonable amounts of phenolic and flavonoid compounds were present in the AB AgNPs mix. According to the previous study performed in our laboratory the TPC and TFC of *A. ampeloprasum* aqueous extract was reported as 14.35 ± 0.01 mg GAE/g ($y = 0.0078x + 0.073$; $R^2 = 0.98$) and 19.83 ± 0.02 mg QE/g ($y = 0.0056x + 0.1939$; $R^2 = 0.98$) respectively (Nallal et al., 2020). The TPC and TFC values obtained for the AB AgNPs were less when compared to the values obtained for the plant extract. Table 1 showed that the TPC and TFC of AB AgNPs

Table 1
Total phenol and flavonoid content of AgNPs synthesized using *A. ampeloprasum* bulbs.

Content	**AB AgNPs**				
	2 μg/ml	4 μg/ml	6 μg/ml	8 μg/ml	10 μg/ml
TPC(mg GAE/g)[a]	0.57 ± 0.01	0.72 ± 0.4	0.31 ± 0.07	1.09 ± 1	1.23 ± 0.04
TFC(mg QE/g)[a]	0.21 ± 1.2	0.43 ± 2.3	0.89 ± 0.2	0.143 ± 0.03	0.197 ± 0.02

Expressed as Mean values (n = 3) ± standard error.

was concentration dependent. The highest TPC (1.23 ± 0.04 mg GAE/g) was obtained for AB AgNPs at a concentration of 10 μg/mL (y = 0.0119x + 0.104; R^2 = 0.99) and TFC at 10 μg/mL concentration was 0.197 ± 0.02 mg QE/g (y = 0.0214x + 0.094; R^2 = 0.98).

3.4. Free radical scavenging activity and antioxidant activity of AB AgNPs

Fig. 6 shows the free radical scavenging ability of AB AgNPs. Previous reports from our laboratory suggest that *A. ampeloprasum* extract was highly efficient in scavenging DPPH radicals (Nallal et al., 2020). Similar efficiency was observed for AB AgNPs from the results of the present study. Fig. 6 shows that AB AgNPs are highly proficient in scavenging DPPH free radicals and the lowest IC_{50} value (8.93 ± 0.2 μg/ mL) was obtained for this assay. AB AgNPs were also efficient in scavenging ABTS•+, H_2O_2, NO and O_2^- radicals and the IC_{50} values of 18.31 ± 0.01, 11.25 ± 0.1, 16.51 ± 0.3 and 23.22 ± 0.07 μg/ mL were obtained for the assays respectively. The scavenging ability of the AB AgNPs was concentration-dependent. The IC_{50} values obtained for Ascorbic acid was lower than the values obtained for AB AgNPs in all the free radical scavenging assays except DPPH assay. The metal chelating ability of AB AgNPs was 53.22 ± 0.2 mg EDTAE/g and the total antioxidant capacity as evaluated by phosphomolybdenum assay was 61.7 ± 1.3 mg AAE/g at 10 μg/mL concentration (Table 2). Ascorbic acid exhibited higher metal chelating ability (264.36 ± 0.03 mg EDTAE/g) at the same concentration.

3.5. Anticandida activity of AB AgNPs

The inhibitory activity of AB AgNPs on the tested candida strains are represented in Fig. 7. The results revealed that AB AgNPs were potentially effective in suppressing the growth of multidrug resistant Candida strains that are harmful human pathogens. The anticandida activity was observed for the strains in the order of susceptibility as follows: *C. albicans* ≥ *C. tropicalis* ≥ *C. glabrata* ≥ *C. parapsilosis* ≥ *C. krusei*. It is elucidated from the results that *C. albicans* was highly susceptible to AB AgNPs at a concentration of 25 μg /mL. The anticandida activity was concentration dependent, at higher concentration of AB AgNPs the zone of inhibition increased.

4. Discussion

The present study elucidated an eco-friendly, cost-effective synthesis of AgNPs assisted by solar radiation. Two mechanisms can be collectively proposed for the immediate synthesis of AgNPs, (i) the intensity of UV solar radiation proportionally increases with increase in altitude. Since the study laboratory is located at Kodaikanal (elevation: 2133 m), a hill station at India, it receives approximately 20 times greater UV radiation than the sea level due to the atmosphere transparency (Dong et al., 2004), (ii) Sunlight irradiations act as catalyst in driving the electron transfer process, mediated by the metabolites and proteins present in the plant extract that stimulates the reduction reaction to occur within few minutes (Ahmed et al., 2015). Collectively, high altitude, high intensity of UV radiation and phytocompounds facilitate the safe, non-toxic and facile reduction of $AgNO_3$ to AgNPs (Fig. 8).

Characterization results of the obtained particles indicated the efficient synthesis of AgNPs. The obtained results of UV–Vis spectroscopy studies were parallel to the results of Abdel-Aziz et al., (2014) who reported the absorption peak (440 nm) for AgNPs synthesized form *Chenopodium murale* leaf extract. Fattorusso et al., (2001) reports Quercetin and Kaempferol as the important flavonoids in *A. ampeloprasum*, which suggests that the flavonoids in the bulbs extract aid in the reduction of Ag ions. Allium species are acknowledged for their organosulphur compounds that contain sulfoxides and thiol groups. It is suggested from the FTIR spectrum that the phenols, flavonoids and sulphur groups present in the bulbs extract act as a reducing and capping agent for the synthesis

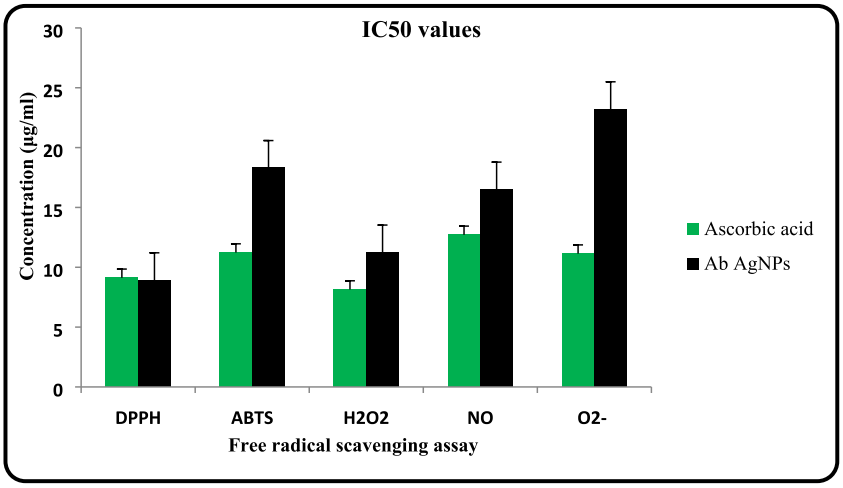

Fig. 6. Comparison of IC_{50} values obtained for Ascorbic acid and AB AgNPs in different free radical scavenging assays.

Table 2
Metal chelating ability and total antioxidant capacity of AB AgNPs.

Assay	AB AgNPs				
	2 µg/ml	4 µg/ml	6 µg/ml	8 µg/ml	10 µg/ml
Metal chelating (mg EDTAE/g)	12.36 ± 0.04	18.42 ± 2.1	29.84 ± 0.7	41.29 ± 1.3	53.22 ± 0.2
Phosphomolybdenum (mg AAE/g)	9.61 ± 0.3	14.24 ± 1.4	25.07 ± 0.01	36.55 ± 0.03	61.7 ± 1.3

Expressed as Mean values (n = 3) ± standard error.

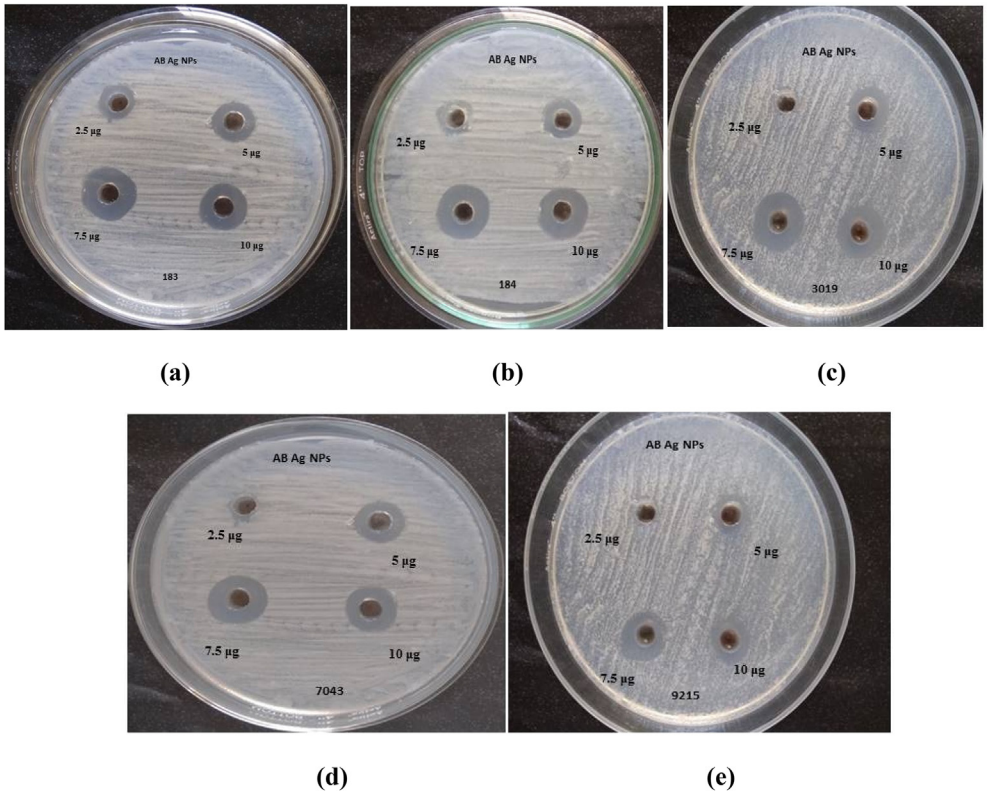

Fig. 7. Anti-candida activity of AB AgNPs against (a) *C. albicans*, (b) *C. topicalis*, (c) *C. glabrata*, (d) *C. parapsilosis*, (e) *C. krusei*.

of AgNPs. Organosulphur compounds also provide reactive functional sites for photochemical changes empowering the rapid reduction of Ag ions on exposure to sunlight irradiation (Toh et al., 2014; Padmos and Zhang, 2012). AgNPs synthesized from *Averrhoa carambola* leaf extract and *Ocimum sanctum* leaf extract showed similar FCC structure obtained from the XRD analysis of the present study (Gavade et al., 2015; Ramteke et al., 2013). The negative potential charge observed in the zeta potential analysis might be contributed by the secondary metabolites such as flavonoids, phenols and saponins that carry negative charges, also primarily due to the organo sulphur compounds in the extracts. This negative potential facilitates the repulsion between each other which prevents the agglomeration/aggregation of the AB AgNPs and provides stability to the particles (Kumar and Dixit, 2017; Teles et al., 2018). Khoshnamvand et al., (2019) reported the zeta potential of AgNPs synthesized from *A. ampeloprasum* leaves to be negative which was similar to our study and suggests the role of plant metabolites for the obtained negative charge. Interestingly, ellipsoidal, triangular and hexagonal shapes (Fig. 5) were also observed which were in agreement with the results of the AgNPs synthesized from *A. ampeloprasum* leaves extract (Khoshnamvand et al., 2019).

Results from the quantitative determination of phytoconstituents were parallel to the results of Firoozi et al., 2016, the TPC and TFC of AgNPs synthesized from *Satureja intermedia* were less when compared to the values obtained for the same plant extract. Higher phenolic and flavonoid content in the plant sample is correlated to the antioxidant capacity of the plant extract. It is plausible that the phytocompounds that act as reducing and capping agents in AB AgNPs synthesis attribute for the antioxidant and free radical scavenging activity. The chemical structure of the polyphenols depict them as strong antioxidant agents since the hydroxyl groups present in the polyphenols can act as hydrogen donors that effectively scavenge the free radicals. Flavonoids are also reported to nullify the effect of free radicals by acting as antiradical agents (Salari et al., 2019; Mohanta et al., 2017). The results of Firoozi et al., 2016 were parallel to our results and the free radical scavenging activity of the AgNPs increased with the increase in the concentration. Results obtained from the agar well diffusion assay was similar to the results of Gudikandula and Maringanti (2016) who reported that biologically synthesized nanoparticles had efficient antimicrobial activity when compared to chemically synthesized AgNPs. Gomaa (2017) reported that AgNPs synthesized using *A. cepa* extract showed a 14 mm inhibition zone against *C. albicans*. AgNPs synthesized from *A. ampeloprasum* leaves inhibited the growth of fungi such as *A. flavus* (8 mm), *A. parasiticus* (10.33 mm), *A. ochraceus* (10.61 mm) and *A. niger* (14 mm) at 652 µg/mL concentrations and above. Additionally,

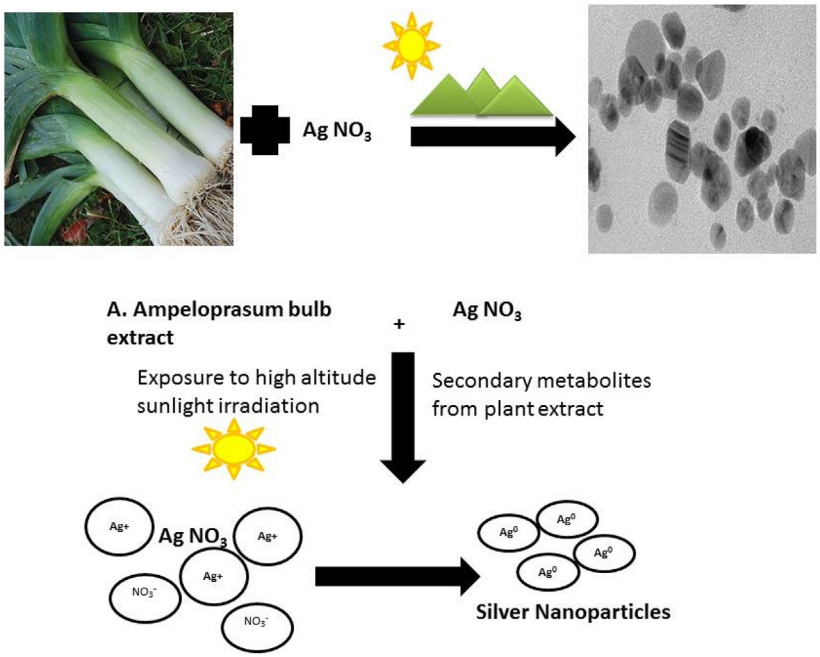

Fig. 8. Mechanism of sunlight-driven AgNP synthesis using *A. ampeloprasum* bulbs extract.

results obtained by Paul et al., (2018) showed that AgNPs synthesized from Curcumin tested against Candida strains were found to have the following inhibition zones: *C. albicans* (20.1 mm), *C. glabrata* (20.6 mm), *C. krusei* (15.1 mm), *C. tropicalis* (16.4 mm) and *C. parapsilosis* (18.4 mm). The MIC of AB AgNPs for *C. albicans* was determined as 32.64 ± 2.1 μg/mL. The result from our previous study showed that 33 ± 2.9 μg/mL of *A. ampeloprasum* aqueous extract was the minimum concentration required to inhibit 75% growth of *C. glabrata* which was the least susceptible organism in the study. The plausible mechanism by which the AgNPs interrupt the candida cell metabolism primarily at cidal or static levels are suggested as (i) disruption of cell wall and the plasma membrane, (ii) increased production of reactive oxygen species at toxic levels to the candida cells (iii) interference with the central dogma of the candida cells (Prabhu and Poulose, 2012). Additionally most enzymes present in the candida cells contain active S-H groups, AgNPs thus can combine with the substrates through competitive inhibition thereby inactivating the enzymes as well as product formation that is necessary for the cell function. FTIR analysis of the AB AgNPs revealed the presence of sulphur groups such as S═O, the capping of these groups on the AgNPs may cause the oxidation of the vital thiol groups in the cell proteins into disulphide groups thus inactivating the enzymes (Ghannoum, 1988).

5. Conclusion

The present study demonstrated a eco-friendly, non-toxic, affordable and facile approach to synthesize AgNPs using *A. ampeloprasum* bulbs extract induced by high altitude sunlight irradiation. FTIR analysis revealed the role of phytocompounds as strong reducing and capping agents in the synthesize process. The negative zeta potential obtained for the AB AgNPs suggested the non-agglomerating tendency of the particles and extended shelf-life with stability. The study suggests that AB AgNPs possess effective antioxidant and free radical scavenging ability that was evaluated using seven *in-vitro* assays. The anticandida activity of the AB AgNPs were impressive though higher concentrations were required to inhibit the candida strains when compared to the standard antifungal agent. Briefly, since *A. ampeloprasum* is an edible plant, AgNPs synthesized from its extract are highly safe and can be used as a promising candidate in modern medicine.

Declaration of Competing Interest

The authors declare that there is no conflict of interest

Acknowledgement

The authors gratefully acknowledge the DST-SERB -Project Ref. No. SB/EMEQ-431/2014, Department of Science and Technology, New Delhi, India. The authors extend their appreciation to Taif University for funding current work by Taif University Researchers Supporting Project number (TURSP-2020/295), Taif University, Taif, Saudi Arabia. This work was also supported by the National Research Foundation of Korea Grant funded by the Korean Government (Ministry of Science and ICT ~ MSIT) (2020R1G1A1012069).

References

Abbas, M.A., 2019. Analgesic effect of Allium ampeloprasum: Evidence for the involvement of beta-adrenergic system. J. Funct. Foods 57, 1–6. https://doi.org/10.1016/j.jff.2019.03.046.

Abdel-Aziz, M.S., Shaheen, M.S., El-Nekeety, A.A., Abdel-Wahhab, M.A., 2014. Antioxidant and antibacterial activity of silver nanoparticles biosynthesized using Chenopodium murale leaf extract. J. Saudi Chem. Soc. 18, 356–363. https://doi.org/10.1016/j.jscs.2013.09.011.

Adão, C.R., Da Silva, B.P., Parente, J.P., 2011. A new steroidal saponin with anti-inflammatory and antiulcerogenic properties from the bulbs of Allium ampeloprasum var. porrum. Fitoterapia 82, 1175–1180.

Ahmed, K.B.A., Senthilnathan, R., Megarajan, S., Anbazhagan, V., 2015. Sunlight mediated synthesis of silver nanoparticles using redox phytoprotein and their application in catalysis and colorimetric mercury sensing. J. Photochem. Photobiol., B 151, 39–45. https://doi.org/10.1016/j.jphotobiol.2015.07.003.

Ahmed, S., Ahmad, M., Swami, B.L., Ikram, S., 2016. A review on plants extract mediated synthesis of silver nanoparticles for antimicrobial applications: A green expertise. J. Adv. Res. 7, 17–28. https://doi.org/10.1016/j.jare.2015.02.007.

Al-Huqail, A.A., Hatata, M.M., Al-Huqail, A.A., Ibrahim, M.M., 2018. Preparation, characterization of silver phyto nanoparticles and their impact on growth potential of Lupinus termis L. seedlings. Saudi J. Biol. Sci. 25, 313–319. https://doi.org/10.1016/j.sjbs.2017.08.013.

Amalraj, S., Krupa, J., Sriramavaratharajan, V., Mariyammal, V., Murugan, R., Ayyanar, M., 2020. Chemical characterization, antioxidant, antibacterial and enzyme inhibitory properties of Canthium coromandelicum, a valuable source for bioactive compounds. J. Pharm. Biomed. Anal. 192,. https://doi.org/10.1016/j.jpba.2020.113620 113620.

An, X., Zhang, X., Yao, H., Li, H., Ren, J., 2015. Effects of diallyl disulfide in elephant garlic extract on breast cancer cell apoptosis in mitochondrial pathway. J. Food Nutrit. Res. 3, 196–201.

Balouiri, M., Sadiki, M., Saad, I., 2015. Methods for *In vitro* evaluating antimicrobial activity: A review. J. Pharm. Anal. 6, 71–79.

Bareemizadeh, F., Ghasempour, H., Maassoumi, S.M., Karimi, N., Taran, M., Ghasempour, M., 2014. In vitro antimicrobial activity of Allium ampeloprasum L. var. atroviolaceum Regel. Int. J. Biosci. 4, 80–84.

Ceccanti, C., Rocchetti, G., Lucini, L., Giuberti, G., Landi, M., Biagiotti, S., Guidi, L., 2020. Comparative phytochemical profile of the Elephant garlic (Allium ampeloprasum var. holmense) and the common garlic (Allium sativum) from the Val di Chiana area (Tuscany, Italy) before and after in vitro gastrointestinal digestion. Food Chem. 338 (128011). https://doi.org/10.1016/j.foodchem.2020.128011.

Chang, C.C., Yang, M.H., Wen, H.M., Chern, J.C., 2002. Estimation of Total Flavonoid Content in Propolis by Two Complementary Colorimetric Methods. J. Food Drug Anal. 10, 178–182.

Dong, S., Tang, C., Zhou, H., Zhao, H., 2004. Photochemical synthesis of gold nanoparticles by the sunlight radiation using a seeding approach. Gold Bull. 37, 187–195. https://doi.org/10.1007/BF03215212.

Fattorusso, E., Lanzotti, V., Scafatu, O.T., Cicala, C., 2001. The flavonoids of leek, Allium porrum. Phytochemistry 57, 565–569. https://doi.org/10.1016/S0031-9422(01)00039-5.

Firoozi, S., Jamzad, M., Yari, M., 2016. Biologically synthesized silver nanoparticles by aqueous extract of Satureja intermedia C.A. Mey and the evaluation of total phenolic and flavonoid contents and antioxidant activity. J. Nanostruct. Chem. 6, 357–364. https://doi.org/10.1007/s40097-016-0207-0.

Gavade, M.S.J., Nikam, G.H., Dhabbe, R.S., Sabale, S.R., Tamhankar, B.V., Mulik, G.N., 2015. Green synthesis of silver nanoparticles by using carambola fruit extract and their antibacterial activity. Adv. Nat. Sci.: Nanosci. Nanotechnol. 6,. https://doi.org/10.1088/2043-6262/6/4/045015 045015.

Ghannoum, M.A., 1988. Studies on the anticandidal mode of action of Allium sativum (garlic). J. Gen. Microbiol. 134, 2917–2924. https://doi.org/10.1099/00221287-134-11-2917.

Gomaa, E.Z., 2017. Antimicrobial, antioxidant and antitumor activities of silver nanoparticles synthesized by Allium cepa extract: A green approach, J. Genetic Eng. Biotechnol 15, 49-57. doi: 10.1016/j.jgeb.2016.12.002.

Gudikandula, K., Maringanti, S.C., 2016. Synthesis of silver nanoparticles by chemical and biological methods and their antimicrobial properties. J. Exp. Nanosci. 11, 714–721. https://doi.org/10.1080/17458080.2016.1139196.

Haq, I., Ullah, N., Bibi, G., Kanwal, S., Ahmad, M.S., Mirza, B., 2012. Antioxidant and Cytotoxic activities and phytochemical analysis of Euphorbia wallichii root extract and its fractions. Iranian J. Pharmacol. Res. 11, 241–249.

Khoshnamvand, M., Huo, C., Liu, J., 2019. Silver nanoparticles synthesized using Allium ampeloprasum L. leaf extract: characterization and performance in catalytic reduction of 4-nitrophenol and antioxidant activity. J. Mol. Struct. 1175, 90–96. https://doi.org/10.1016/j.molstruc.2018.07.089.

Krishna, M.I., Reddy, B.G., Veerabhadram, G., Madhusudhan, A., 2015. Eco-friendly green synthesis of silver nanoparticles using salmalia malabarica: synthesis, characterization, antimicrobial, and catalytic activity studies. Appl. Nanosci. 6, 681–689. https://doi.org/10.1007/s13204-015-0479-6.

Kumar, A., Dixit, C.K., 2017. Methods for characterization of nanoparticles. Adv. Nanomed. Delivery Therap. Nucl. Acids 2017, 43–58. https://doi.org/10.1016/B978-0-08-100557-6.00003-1.

Lu, X., Ross, C.F., Powers, J.R., Aston, D.E., Rasco, B.A., 2011. Determination of total phenolic content and antioxidant activity of Garlic (Allium sativum) and Elephant Garlic (Allium ampeloprasum) by attenuated total reflectance–fourier transformed infrared spectroscopy. J. Agric. Food. Chem. 59, 5215–5221.

Mallmann, E.J., Cunha, F.A., Castro, B.N., Maciel, A.M., Menezes, E.A., Fechine, P.B., 2015. Antifungal activity of silver nanoparticles obtained by green synthesis. Rev. Inst. Med. Trop. Sao Paulo 57, 165–167. https://doi.org/10.1590/S0036-46652015000200011.

Manzocco, L., Anese, M., Nicoli, M.C., 1998. Antioxidant properties of tea extracts as affected by processing. Lebens-mittel-Wissenschaft Und-Technologies 31, 694–698.

Mohanta, Y.K., Panda, S.K., Jayabalan, R., Sharma, N., Bastia, A.K., Mohanta, T.K., 2017. Antimicrobial, Antioxidant and Cytotoxic Activity of Silver Nanoparticles Synthesized by Leaf Extract of Erythrina suberosa (Roxb.). Front. Mol. Biosci. 4, 14. https://doi.org/10.3389/fmolb.2017.00014.

Najda, A., Błaszczyk, L., Winiarczyk, K., Dyduch, J., Tchorzewska, D., 2016. Comparative studies of nutritional and health-enhancing properties in the "garliclike" plant Allium ampeloprasum var. ampeloprasum (GHG-L) and A. sativum. Sci. Hortic. 201, 247–255.

Nallal, V.U.M., Padmini, R., Ravindran, B., Chang, S.W., Radhakrishnan, R., Almoallim, H.S.M., Alharbi, S.A., Razia, M., 2020. Combined in vitro and in silico approach to evaluatethe inhibitory potential of an underutilized allium vegetable and its pharmacologically active compounds on multidrug resistant Candida species. Saudi J. Biol. Sci. 28, 1246–1256. https://doi.org/10.1016/j.sjbs.2020.11.

Padmos, J.D., Zhang, P., 2012. Surface Structure of Organosulfur Stabilized Silver Nanoparticles Studied with X-ray Absorption Spectroscopy. J. Phys. Chem. C 116, 23094–23101. https://doi.org/10.1021/jp3075332.

Paul, S., Mohanram, K., Kannan, I., 2018. Antifungal activity of curcumin-silver nanoparticles against fluconazole-resistant clinical isolates of Candida species. Pharm. Study 39, 182–186.

Prabhu, S., Poulose, E.K., 2012. Silver nanoparticles: mechanism of anti -microbial action, synthesis, medical applications, and toxicity effects. Int. Nano Lett. 2, 32. https://doi.org/10.11186/2228-5326-2-32.

Prieto, P., Pineda, M., Aguilar, M., 1999. Spectrophotometric quantitation of antioxidant capacity through the formation of a phosphomolybdenum complex: specific application to the determination of vitamin E. Anal. Biochem. 269, 337–341.

Rahimi-Madiseh, M., Heidarian, E., Kheiri, S., Rafieian-Kopaei, M., 2017. Effect of hydroalcoholic Allium ampeloprasum extract on oxidative stress, diabetes mellitus and dyslipidemia in alloxan-induced diabetic rats. Biomed. Pharmacother. 86, 363–367.

Ramteke, C., Chakrabarti, T., Sarangi, B.K., Pandey, R.-A., 2013. Synthesis of Silver Nanoparticles from the Aqueous Extract of Leaves ofOcimum sanctumfor Enhanced Antibacterial Activity. J. Chem. 2013, 1–7. https://doi.org/10.1155/2013/278925.

Ruch, R.J., Cheng, S.J., Klaunig, J.E., 1989. Prevention of cytotoxicity and inhibition of intercellular communication by antioxidant catechins isolated from Chinese green tea. Carcinogen 10, 1003–1008.

Saha, M., Bandyopadhyay, P.K., 2017. Green Biosynthesis of Silver Nanoparticle Using Garlic, Allium sativum with Reference to Its Antimicrobial Activity against the Pathogenic Strain of Bacillus sp. and Pseudomonas sp. Infecting Goldfish, Carassiusauratus. ProcZoolSoc 1-7. doi: 10.1007/s12595-017-0258-3 2017

Salari, S., Esmaeilzadeh Bahabadi, S., Samzadeh-Kermani, A., Yosefzaei, F., 2019. In-vitro Evaluation of Antioxidant and Antibacterial Potential of GreenSynthesized Silver Nanoparticles Using Prosopis farcta Fruit Extract. Iranian J. Pharm. Res.: IJPR 18, 430–455.

Saravanan, C., Rajesh, R., Kaviarasan, T., Muthukumar, K., Kavitake, D., Shetty, P.H., 2017. Synthesis of silver nanoparticles using bacterial exopolysaccharide and its application for degradation of azo-dyes. Biotechnol. Rep, 15, 33–40. https://doi.org/10.1016/j.btre.2017.02.006.

Seeram, N.P., Henning, S.M., Lee, R., Niu, Y., Scheuller, H.S., 2006. Catechin D. and caffeine contents of green tea dietary supplements and correlation with antioxidant activity. J. Agric. Food Chem. 54, 1599–1603.

Shah, M., Nawaz, S., Jan, H., Uddin, N., Ali, A., Anjum, S., Giglioli–Guivarch'h N., Hano C., Abbasi, B. H. (2020). Synthesis of bio-mediated silver nanoparticles from Silybum marianum and their biological and clinical activities. Mater. Sci. Eng.: C, 110889. doi:10.1016/j.msec.2020.110889

Sobolewska, D., Michalska, K., Podolak, I., Grabowska, K., 2014. Steroidal saponins from the genus Allium. Phytochem. Rev. 15, 1–35. https://doi.org/10.1007/s11101-014-9381-1.

Teles, Y., Souza, M., Souza, M., 2018. Sulphated Flavonoids: Biosynthesis, Structures, and Biological Activities. Molecules 23, 480. https://doi.org/10.3390/molecules23020480.

Toh, H.S., Batchelor-McAuley, C., Tschulik, K., Compton, R.G., 2014. Chemical interactions between silver nanoparticles and thiols: a comparison of mercaptohexanol against cysteine. Sci. China Chem. 57, 1199–1210. https://doi.org/10.1007/s11426-014-5141-8.